Radiation Protection Strategy Development for Mars Surface Exploration

Arturo R. Ortiz[1], Vadim Y. Rygalov[2], and Pablo de León[3]
University of North Dakota, Grand Forks, ND, 58202

Computational analyses were performed to assess space radiation shielding effectiveness of 'minimal' planetary surface exploration concepts developed by the University of North Dakota: the Inflatable Lunar-Martian Habitat (ILMH), Pressurized Electric Rover (PER), and NDX-2 space suit. Using the HZETRN and NUCFRG3 radiation analysis computer codes with ray-by-ray transport through three-dimensional shielding thickness distributions, the authors calculated doses in the Mars surface environment under conditions of the February 1956 solar flare and 1977 solar minimum galactic cosmic radiation. Results indicate that polyethylene shielding of 5, 10, and 15 g/cm^2 can protect the ILMH up to 11, 18, and 25 km surface elevation, respectively, while 1m of Mars regolith can protect up to 30 km. The shielded ILMH is adequate as primary radiation storm shelter, and meets permissible limits for 30 and 365 day exposures. The structural shell of the PER can protect from acute exposure only up to 5 km elevation, and hence is not adequate as a secondary storm shelter. A Mylar space suit at a thickness of 500 micrometers can protect from acute exposure only up to 4 km. The authors estimated doses for surface stays of 365 days, and found total dose varied from 176 mGy-Eq while performing minimal exploration, to 1025 mGy-Eq in a scenario that includes extravehicular activity (EVA) between 24 and 30 km elevation during a large solar flare. Acute exposure during the flare at high surface elevation approaches the threshold for acute radiation syndrome. Since the PER and space suit cannot protect from short term exposure except over a limited elevation range, fast access to a shielded habitat will always be required if a major solar storm occurs during surface roving or EVA. This drives a need to implement an early warning system for solar storms to enable safe extended surface exploration of Mars.

Nomenclature

AU	=	astronomical unit
BFO	=	blood forming organs
CNS	=	central nervous system
EVA	=	extravehicular activity
GCR	=	galactic cosmic radiation
HZETRN	=	High Charge (Z) and Energy Transport
ILMH	=	Inflatable Lunar-Martian Habitat
mGy-Eq	=	milli Gray equivalent
NDX	=	North Dakota Experimental
NUCFRG	=	Nuclear Fragmentation
OLTARIS	=	On Line Tool for the Assessment of Radiation in Space
PEL	=	Permissible Exposure Limit
PER	=	Pressurized Electric Rover
SPE	=	solar particle event
UND	=	University of North Dakota
Z	=	atomic number

---

[1] Graduate Student, Department of Space Studies, 4149 University Ave., Stop 9008, Grand Forks, ND 58202

[2] Associate Professor, Department of Space Studies, 4149 University Ave., Stop 9008, Grand Forks, ND 58202

[3] Associate Professor, Department of Space Studies, 4149 University Ave., Stop 9008, Grand Forks, ND 58202

I.   Introduction

Human exploration of Mars will involve surface stays of one Earth year or longer. During an extended stay, the crew may experience a major solar particle event (SPE) in addition to background galactic cosmic radiation (GCR). Since Mars does not have the protection of a planetary magnetosphere, doses of ionizing radiation will be high. The thin Mars atmosphere will provide relatively little protection. Without radiation shielding, Permissible Exposure Limits (PELs)[1,2] will be exceeded. Astronauts will require the protection of a shielded habitat, with very limited protection provided by surface rovers and space suits.

We performed computational analyses to assess radiation doses inside 'minimal' planetary surface exploration concepts developed by the University of North Dakota (UND) under a NASA grant: the Inflatable Lunar-Martian Habitat (ILMH), Pressurized Electric Rover (PER), and the North Dakota Experimental (NDX)-2 space suit. Initially, these concepts were developed to provide minimal life support structures for astronauts. For the ILMH, we examined several shielding configurations and identified surface elevations where the ILMH could be deployed to ensure PELs are met. For the PER, we calculated internal doses under operationally realistic materials and thicknesses. For the space suit, we calculated internal doses under operationally realistic suit fabric and thicknesses. We estimated doses for minimal, intermediate, and extreme surface exploration scenarios.

II.   Method

A. Overview

These investigations used the latest version of the HZETRN (High Charge [Z] and Energy Transport) and NUCFRG3 (Nuclear Fragmentation 3) computer codes, developed by the NASA Langley Research Center, available through the On Line Tool for the Assessment of Radiation in Space (OLTARIS) web site.[3] HZETRN transport algorithms solve numerically the linearized Boltzmann transport equation using Bethe-Bloch theory, along with the straight-ahead and continuous slowing down approximations.[4] The most recent version accounts for neutron backscatter from planetary surfaces. NUCFRG3 analyzes heavy ion collisions using the abrasion-ablation model of heavy ion fragmentation to estimate cross sections for production of isotopes. It computes production cross sections of emerging particles for input into HZETRN.[5-7]

We assumed a worst case external radiation environment. The February 1956 solar flare is considered to be the most severe SPE ever observed.[8] The 1977 solar minimum galactic cosmic radiation (GCR) is considered to be a severe environment.[9] Calculations used the NASA Langley model of the February 1956 solar flare and the Badhwar-O'Neill 2010 model of 1977 solar minimum GCR, in the Mars surface environment of the Mars-GRAM 2001 atmospheric model. Figure 1 shows the proton spectrum generated by HZETRN for the February 1956 solar flare after transport through the Mars atmosphere to 0 km surface elevation, in the external environment. Although other ion species are present in the solar flare, proton fluence is dominant. Figure 2 shows the proton spectrum generated by HZETRN for 1977 solar minimum GCR after transport through the Mars atmosphere to 0 km surface elevation, in the external environment. Although other ion species are present in the GCR, the proton flux is highest. We defined surface environments of acute, 30 day, and 365 day exposure. Acute exposure calculations were used to identify situations where an astronaut could be near the threshold for acute radiation syndrome. Calculations of 30 day and 365 day exposures were used to compare levels to NASA dose limits for short term or career non-cancer effects.

We implemented very simple models of the ILMH, PER, and space suit, for evaluation of internal doses. For each concept, the shielding was represented as a three-dimensional material thickness distribution. Each thickness distribution consists of a 42-ray geodesic sphere centered at interior target points, with a shielding material thickness specified along each ray. The rays are evenly distributed over a full solid angle of 4π steradians, with each ray accompanied by an opposite ray.

B. ILMH

We represented the ILMH as a hollow box of dimensions 12.2 m x 3m x 2.4 m, with no internal shielding, seated on the Martian surface. We examined shielding over the roof and along the four walls, with no floor shielding, assuming the planetary body provides shielding from the floor direction.

For shielding materials, we considered liquid hydrogen, water, graphite epoxy 51-49, polyethylene, and Mars regolith. A preliminary assessment compared the shielding effectiveness of these five materials to aluminum, using HZETRN and NUCFRG3. Figure 3 shows HZETRN results for radiation attenuation by equal masses of these six

materials in the 1977 solar minimum GCR environment at 1 AU. The curves indicate that liquid hydrogen is the strongest attenuator by mass, whereas aluminum is the weakest. Figure 4 shows HZETRN results for radiation attenuation by equal volumes of these materials in the same environment. The curves indicate that aluminum is the strongest attenuator up to a thickness of about 15 cm, and polyethylene is the strongest above 15 cm. Polyethylene and graphite epoxy 51-49 have similar radiation attenuation properties.
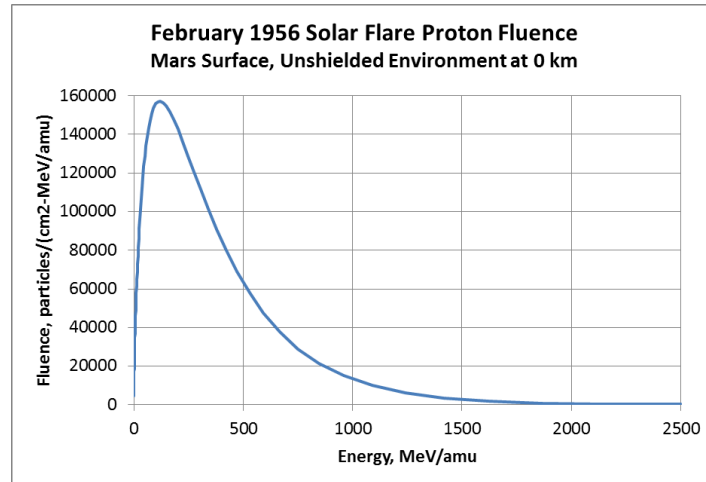
Figure 1. February 1956 solar flare proton fluence on Mars at 0 km in external environment
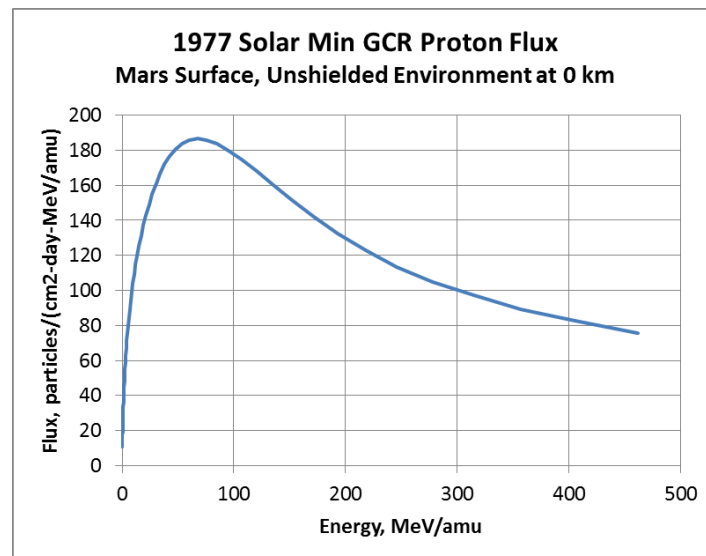
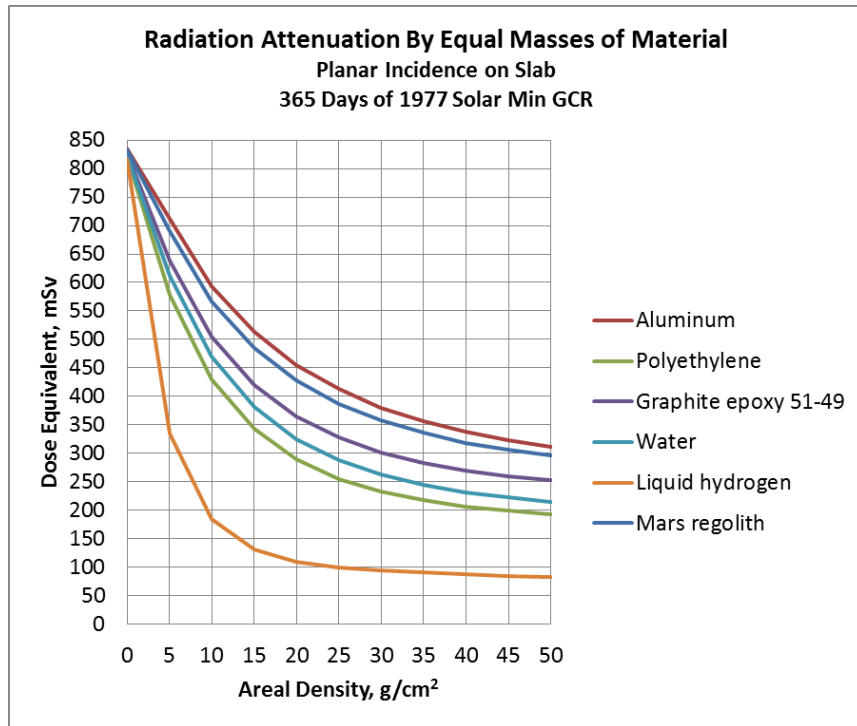**Figure 2. 1977 solar min GCR proton flux on Mars at 0 km in external environment**

Figure 3. Radiation attenuation by equal masses of material
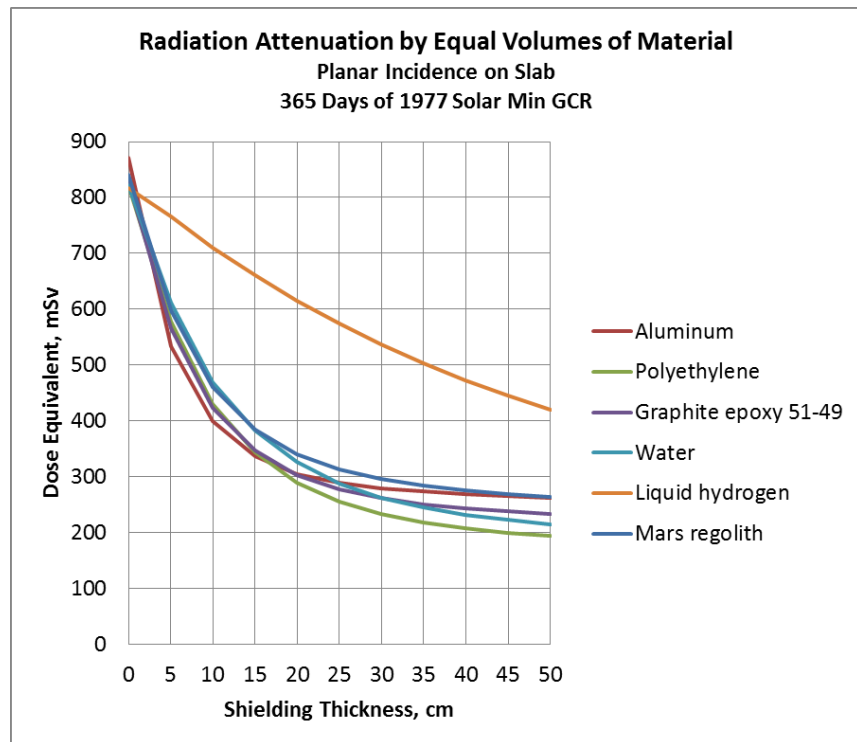

Figure 4. Radiation attenuation by equal volumes of material

Polyethylene represents the best overall compromise between desirable, though somewhat competing attributes of attenuation of high-energy source ions and secondary particles, mass efficiency, volume efficiency, being a light

material that reduces production of secondary particles, hydrogen-rich content, and high number of electrons per unit mass. Hence, we selected polyethylene as the primary shielding material for the ILMH. We selected Mars regolith as a secondary shielding material, in case massive shielding is required. This enables exploitation of a planetary resource, if required.

We defined external surface radiation environments of acute, 30 day, and 365 day exposure, over an elevation range of -10 to 30 km. For each of these environments, we assumed an SPE would occur during the time interval, in addition to background GCR. Table 1 shows our definitions of the surface environments.

Table 1.   Surface environments for exposure inside the ILMH

Exposure	External Environment
Acute	February 1956 solar flare and 1 day of 1977 solar minimum GCR
30 day	February 1956 solar flare and 30 days of 1977 solar minimum GCR
365 day	February 1956 solar flare and 365 days of 1977 solar minimum GCR

C. PER

We represented the PER as a hollow polyhedron of approximate dimensions 4.49 m x 1.42 m x 2.13 m, with no internal shielding, seated on the Martian surface. In this very simple model, shielding is provided only by the external structural materials, with no accounting for internal structures and hardware, cupolas, or suitports. The roof, port, starboard, bow, and stern sides are composed of fiberglass of 0.7 cm thickness, except for windows and a graphite epoxy hatch of 0.7 cm thickness on the port side. The floor is aluminum with a thickness of 0.8 cm. Windows were represented as open areas in the shield with zero shielding thickness. We selected target points in the cockpit and sleep areas, where astronauts are likely to dwell. In the cockpit, we selected two points centered behind the front and side windows, at about where driver and passenger heads would be located, at the port and starboard sides. In the sleep area, we selected five points evenly distributed over the length of port and starboard hammocks installed in the lower aft area of the PER, parallel to the bow-to-stern direction. The target points in the cockpit were selected to maximize radiation exposure due to unshielded windows. The target points in the sleep area are lower in height, farther from the windows, and hence somewhat less exposed. The even distribution of target points in the sleep area over the bow-to-stern direction was selected to find evidence of dose variation between the relatively unshielded cockpit space and the slightly more shielded stern. The goal was to produce data to support recommendations for optimizing the arrangement of the sleep area to minimize radiation exposure. Figure 5 shows the layout of target points on the port side (A) and on the bow (B). Figure 5A also illustrates rays from the port side converging on the port cockpit target point. Table 2 has the coordinates of PER target points in the *xyz* system of Figure 5.

We assumed surface roving could last up to 24 continuous hours, and that an SPE occurs during the 24 hour interval, when the PER and passengers are far from the protection of the ILMH. The time interval of 24 hours is driven by the limited electric power provided by the PER battery before recharging is required. We considered only acute exposure inside the PER, whose external environment we defined as the February 1956 solar flare and one day of 1977 solar minimum GCR, over a surface elevation range of -10 to 30 km.

In anticipation of very little radiation attenuation by the thin PER shell, we also examined an alternative heavy PER, to emphasize sensitivity to shielding thickness. The shell thickness was increased by almost a factor of four across all surfaces, as an upper limit of realistic operational thickness.

D. Space Suit

We represented the space suit as a hollow hemisphere of Mylar fabric seated on the Martian surface, in accordance with the method described by Townsend and colleagues.[10] We evaluated the space suit internal radiation environment at Mylar thicknesses of 50 and 500 micrometers (areal densities of 0.00665 and 0.0665 g/cm^2, respectively). We considered only acute exposure. For an astronaut performing extravehicular activity (EVA) for up to 8 hours outside the protection of a shelter, the external environment for acute exposure was defined as the February 1956 solar flare combined with 8 hours (0.3333 days) of background 1977 solar minimum CGR.
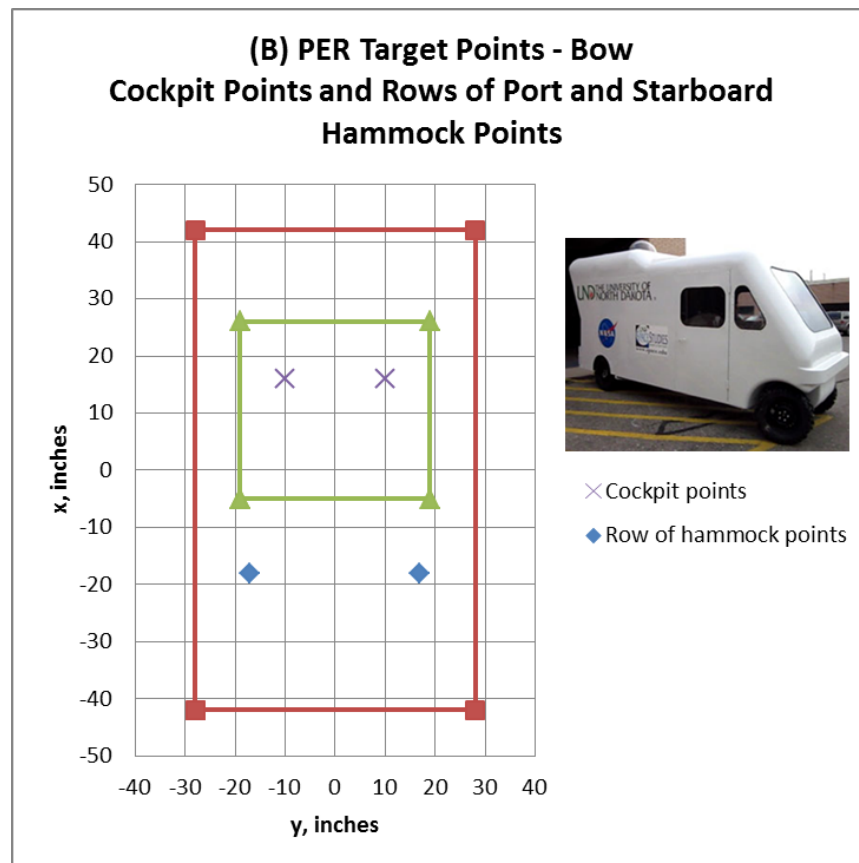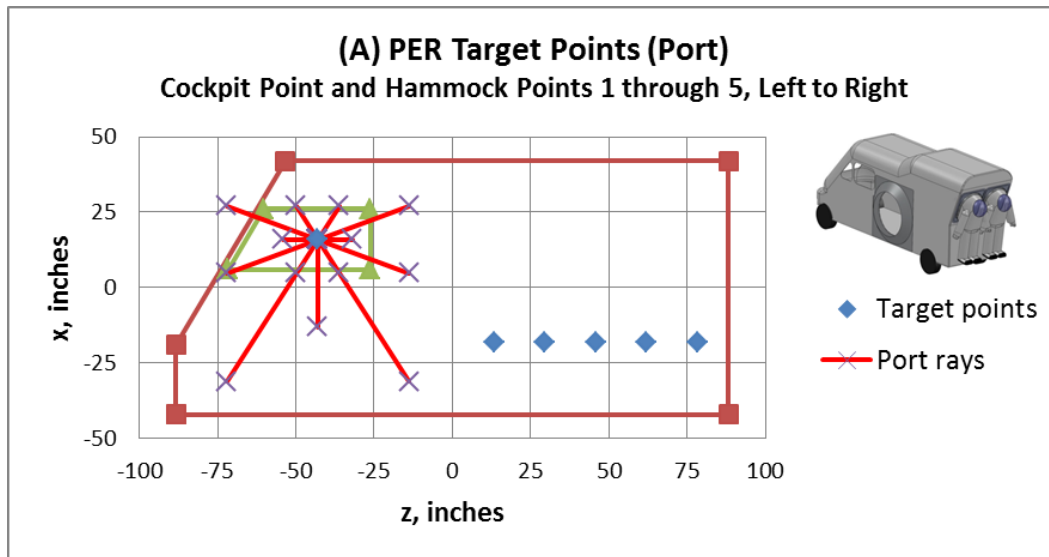
(A) PER Target Points (Port)
Cockpit Point and Hammock Points 1 through 5, Left to Right

(B) PER Target Points - Bow
Cockpit Points and Rows of Port and Starboard Hammock Points

Figure 5. PER target points on port side (A) and bow (B)

Table 2. PER target points (coordinates refer to Figure 5)

Target Point	*x*, inches	*y*, inches	*z*, inches
Port cockpit	16	10	-43
Port hammock 1	-18	17	13.3
Port hammock 2	-18	17	29.55
Port hammock 3	-18	17	45.8
Port hammock 4	-18	17	62.05
Port hammock 5	-18	17	78.3
Starboard cockpit	16	-10	-43
Starboard hammock 1	-18	-17	13.3
Starboard hammock 2	-18	-17	29.55
Starboard hammock 3	-18	-17	45.8
Starboard hammock 4	-18	-17	62.05
Starboard hammock 5	-18	-17	78.3

E. Surface Scenarios

The authors proposed three surface scenarios with a stay of one Earth year. A minimal scenario entails exposure in a relatively benign radiation environment. An intermediate scenario entails moderate exposure, and is more likely to resemble operational conditions on Mars. An extreme scenario entails exposure under worst conditions, possibly leading to acute radiation syndrome. In all three scenarios, the only protection from radiation is provided by either the ILMH shielding, PER shell, or space suit fabric.

In the minimal scenario, the ILMH is deployed at 0 km surface elevation, under polyethylene shielding of 5 g/cm^2 areal density, in the external environment of the February 1956 solar flare and 1977 solar minimum GCR. PER roving occurs under the external radiation environment of background 1977 solar minimum GCR. For PER dwells, we evaluated dose at the relatively exposed port cockpit target point, for conservatism. During EVA, the astronaut is protected only by a space suit made of Mylar fabric of 500 micrometers thickness, while exposed to background 1977 solar minimum GCR. Local EVAs of 3 hours duration occur at 0 km elevation. Short and long excursions of PER roving occur over a surface elevation range of -4 to 4 km. Short excursions last 24 hours, of which 8 are inside the PER and 16 are EVA. Long excursions last 72 hours, of which 24 are inside the PER and 48 are EVA. Each month, the astronaut performs 25 local EVAs, two short roving excursions, and one long roving excursion, with excursion dwell times evenly distributed over the surface elevation range of -4 to 4 km. The environment for acute exposure is the February 1956 solar flare occurring while inside the ILMH under one day of background 1977 solar minimum GCR. Table 3 is a summary of surface activities and environments under the minimal scenario.

Table 3. Minimal surface scenario

Surface Activity	Radiation Shielding	Total Duration (Days)	External Radiation Environment
Local EVA	500 micrometers of Mylar fabric	37.5	1977 solar min GCR at 0 km
Excursion EVAs	500 micrometers of Mylar fabric	40	Average 1977 solar min GCR over -4 to 4 km
Excursion PER dwells	PER structure	20	Average 1977 solar min GCR over -4 to 4 km
ILMH dwell	5 g/cm^2 polyethylene	267.5	February 1956 solar flare and 1977 solar min GCR at 0 km

General conditions for the intermediate and minimal scenarios are similar. The exception is that in the intermediate scenario, the solar flare occurs during EVA at 4 km elevation, instead of while inside the ILMH. Hence, the environment for acute exposure is the February 1956 solar flare while under the protection of the space suit alone at 4 km elevation, under one day of background 1977 solar minimum GCR.

Table 4. Climbing expedition

Surface Activity	Radiation Shielding	Total Duration (Days)	External Radiation Environment
Excursion PER dwells from 0 to 6 km elevation	PER structure	3	Average 1977 solar min GCR from 0 to 6 km
Excursion PER dwells from 6 to 12 km elevation	PER structure	2	Average 1977 solar min GCR from 6 to 12 km
Excursion EVAs from 12 to 18 km elevation	500 micrometers of Mylar fabric	2	Average 1977 solar min GCR from 12 to 18 km
Excursion EVAs from 18 to 24 km elevation	500 micrometers of Mylar fabric	2	Average 1977 solar min GCR from 18 to 24 km
Excursion EVAs from 24 to 30 km elevation	500 micrometers of Mylar fabric	1	February 1956 solar flare and 1977 solar min GCR, both averaged over 24 to 30 km elevation

The extreme scenario includes a 10 day climbing expedition to 30 km elevation. For 11 of the 12 months, general conditions for the extreme scenario are the same as for the minimal scenario, but with no solar flare while inside the ILMH. During the remaining month, the astronaut performs only 10 local EVAs, and does not perform any short or long excursion roving. Instead, the astronaut performs the 10 day climbing expedition up to 30 km elevation under one day of background GCR, with a solar flare occurring during EVA between 24 and 30 km. The environment for acute exposure is the February 1956 solar flare and one day of background 1977 solar minimum GCR, with both the flare and the GCR averaged over 24 to 30 km elevation. Table 4 shows the activities and environments of the climbing expedition.

III. Results

A. ILMH

We calculated internal doses at the center of the ILMH box, under polyethylene layers of 5, 10, and 15 g/cm^2 areal density, and under regolith layers of 1 and 2m thickness. Figures 6 through 8 are surface plots for exposure under polyethylene shielding for 1, 30, and 365 days, respectively. Each surface plot shows dose in the external environment and at shielding of 5, 10, and 15 g/cm^2 areal density. The plots indicate a relatively steep attenuation slope over the first 5 g/cm^2 of polyethylene, with a progressive leveling off up to 15 g/cm^2. This illustrates the diminishing effectiveness of greater shielding thickness, and suggests that addition of another 5 g/cm^2 on top of the 15 g/cm^2 would result in only marginal reduction in dose.

Figures 9 through 11 are the corresponding contour plots. To assess the effectiveness of ILMH shielding, we compared calculated doses to 150 mGy-Eq for acute exposure (1 day), and to NASA dose limits for short term or career non-cancer effects[1] (30 and 365 day). Calculated doses were interpolated to find minimum surface elevations where limits are exceeded. Figure 9 indicates the 1 day dose exceeds 150 mGy-Eq at elevation above 5.2 km in the external environment, above 11.5 km behind 5 g/cm^2 of polyethylene, above 18.0 km behind 10 g/cm^2, and above 25.4 km behind 15 g/cm^2. Figure 10 indicates that the lowest PEL for 30 day exposure, which is 250 mGy-Eq for blood forming organs (BFO) and heart, is exceeded above 12.6 km elevation in the external environment. Figure 10 also indicates this limit is exceeded above 26.4 km behind 5 g/cm^2 of polyethylene. Finally, Figure 10 indicates that all PELs for 30 day exposure are met behind 10 g/cm^2 of polyethylene shielding over the entire surface elevation range of -10 to 30 km. Figure 11 indicates that the lowest PEL for 1 year exposure, which is 500 mGy-Eq for BFO and heart, is exceeded above 17.6 km in the external environment. Figure 11 also indicates that all PELs for 1 year exposure are met behind 5 g/cm^2 of polyethylene shielding over the entire surface elevation range of -10 to 30 km. For incident ions of atomic number $Z \geq 10$, there is a 1 year limit of 100 mGy for the central nervous system (CNS). However, ions of $Z \geq 10$ are more likely to be found in GCR. HZETRN results indicate GCR exposure remains below 100 mGy even in the external environment for 1 year at 30 km elevation. Therefore, we consider this limit as being met.

Figures 12 through 14 are surface plots for exposure under regolith shielding for 1, 30, and 365 days, respectively. Each surface plot shows dose in the external environment and under 1 and 2m of regolith thickness. (The external environment is the same as for polyethylene shielding.) The plots indicate a very steep attenuation slope over the first meter of regolith, with a much lower slope over the second meter. This illustrates the diminishing effectiveness of greater shielding thickness, as similarly illustrated by the surface plots for polyethylene shielding. The plots suggest that addition of a third meter of regolith would result in only marginal reduction in dose. Figures 15 through 17 are the corresponding contour plots. They indicate that 1m of regolith shielding is sufficient to meet a 150 mGy-Eq limit for acute exposure, and PELs for 30 day and 1 year exposure, over the entire surface elevation range of -10 to 30 km.
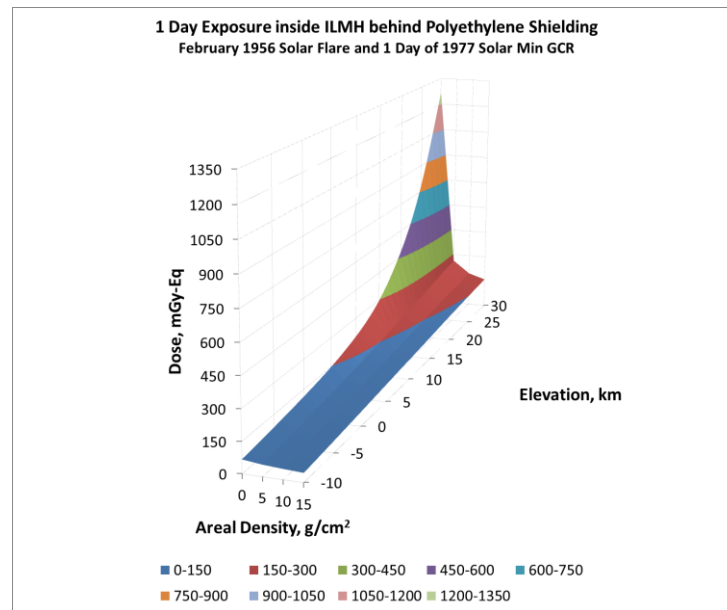
Figure 6. Surface plot of 1 day exposure inside ILMH – polyethylene shielding
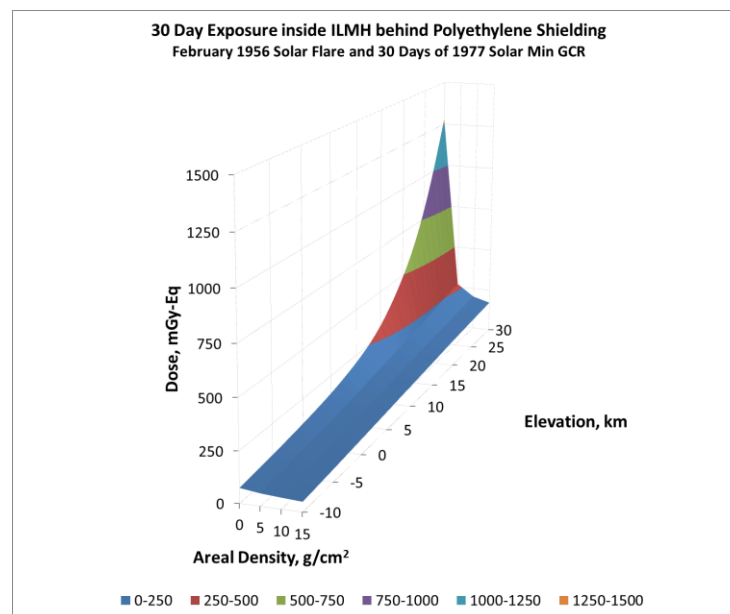
Figure 7. Surface plot of 30 day exposure inside ILMH – polyethylene shielding
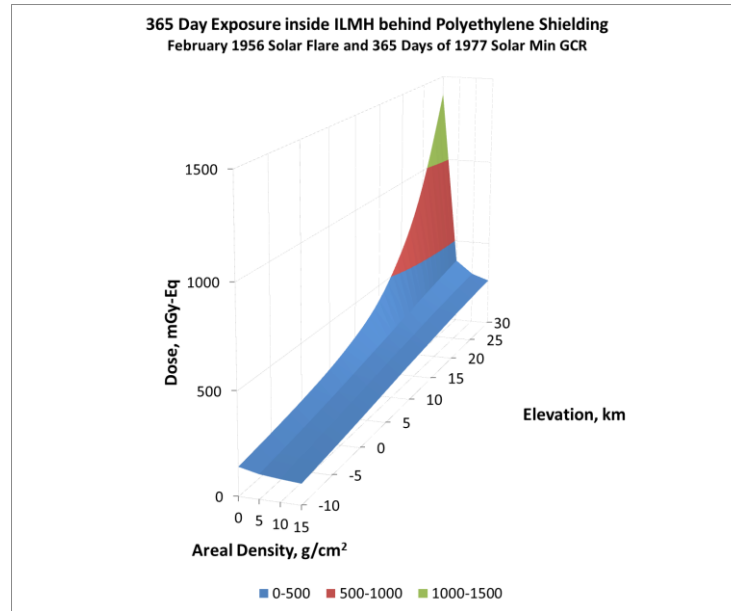
Figure 8. Surface plot of 365 day exposure inside ILMH – polyethylene shielding
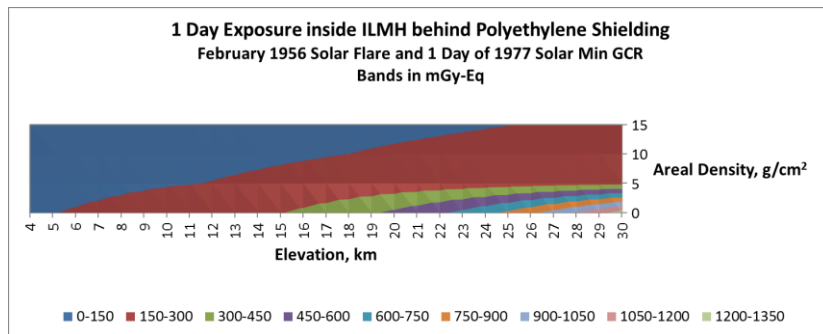

Figure 9. Contour plot of 1 day exposure inside ILMH – polyethylene shielding.
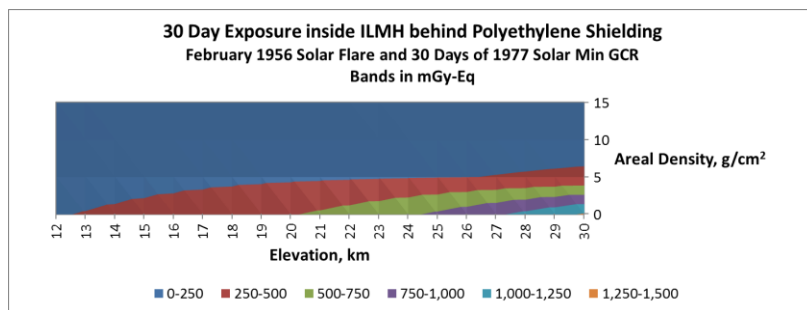

Figure 10. Contour plot of 30 day exposure inside ILMH – polyethylene shielding
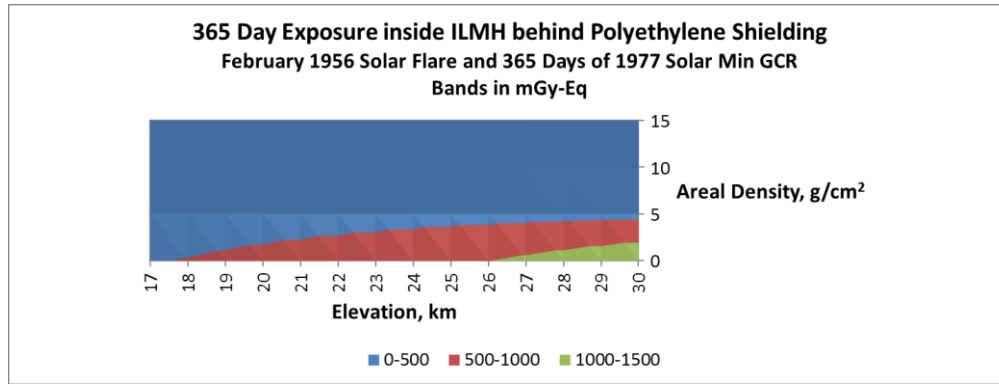
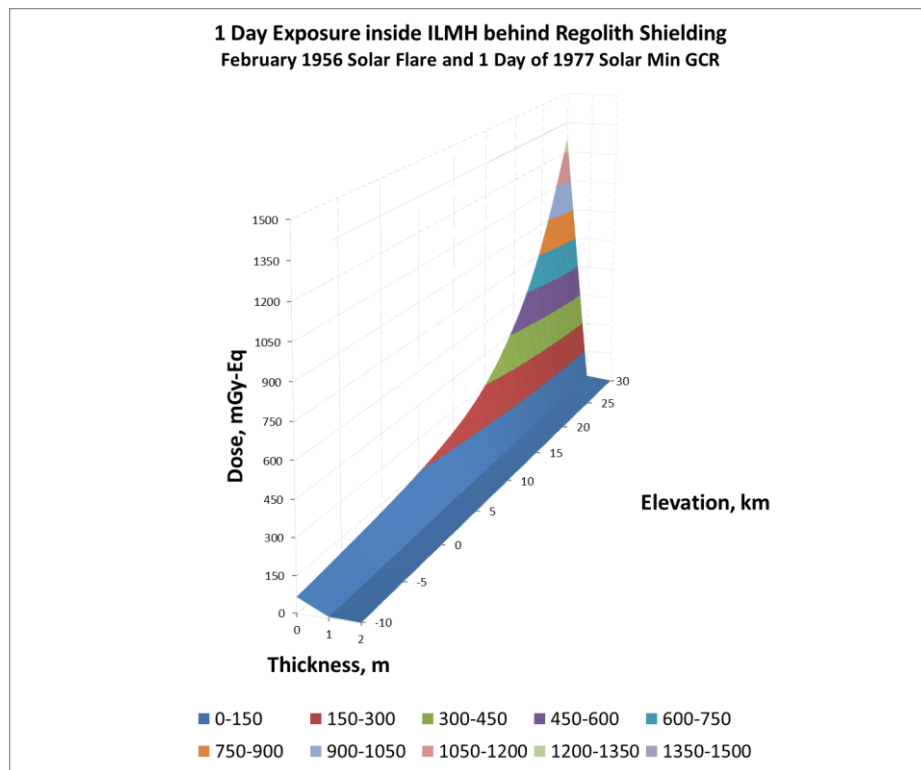**Figure 11. Contour plot of 365 day exposure inside ILMH – polyethylene shielding**

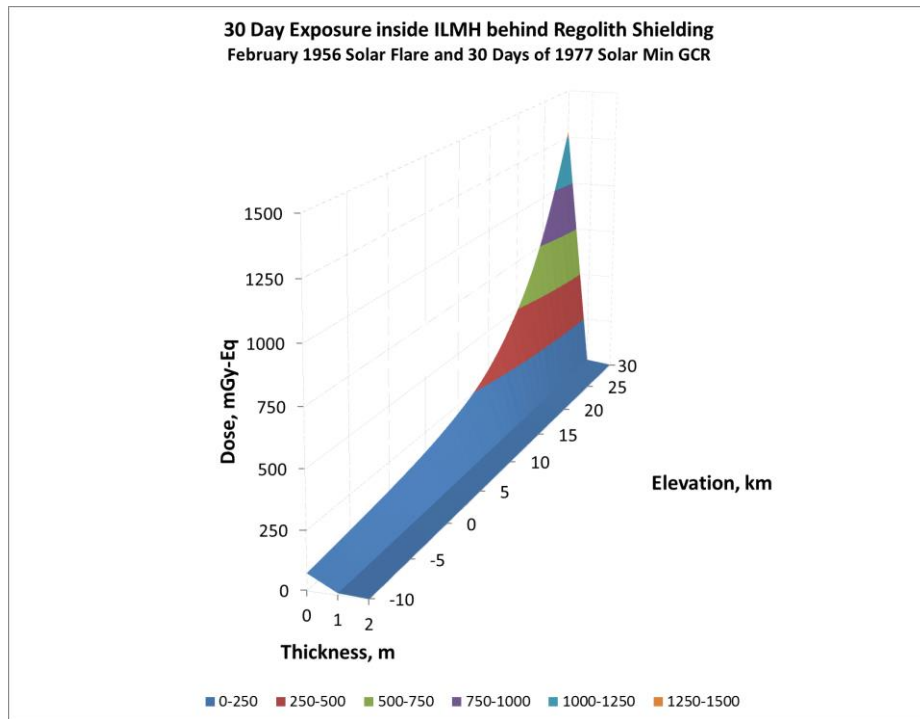**Figure 12. Surface plot of 1 day exposure inside ILMH – regolith shielding**

Figure 13. Surface plot of 30 day exposure inside ILMH – regolith shielding
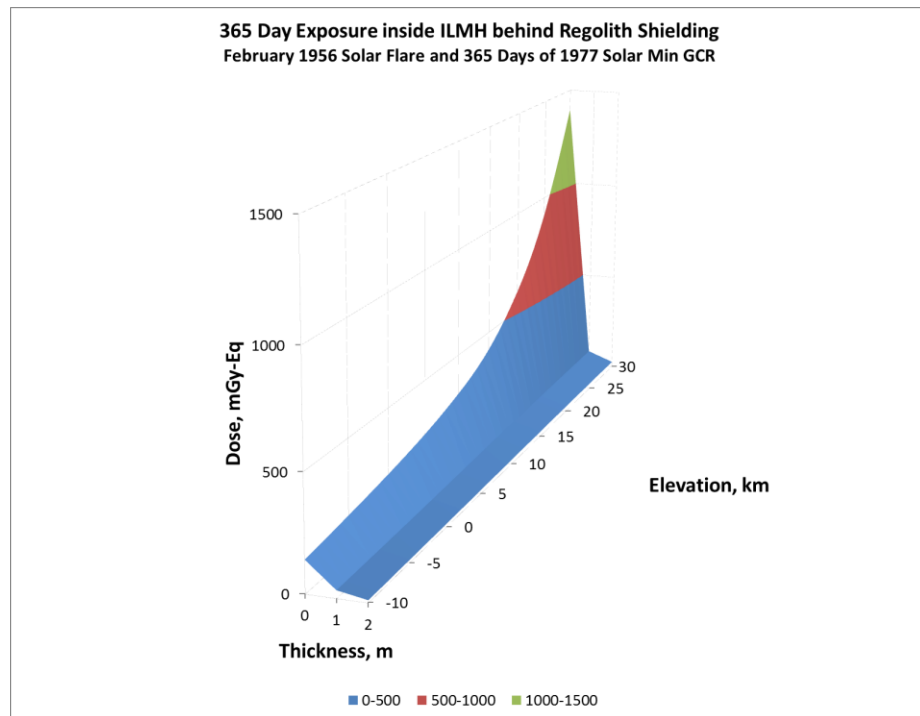

Figure 14. Surface plot of 365 day exposure inside ILMH – regolith shielding

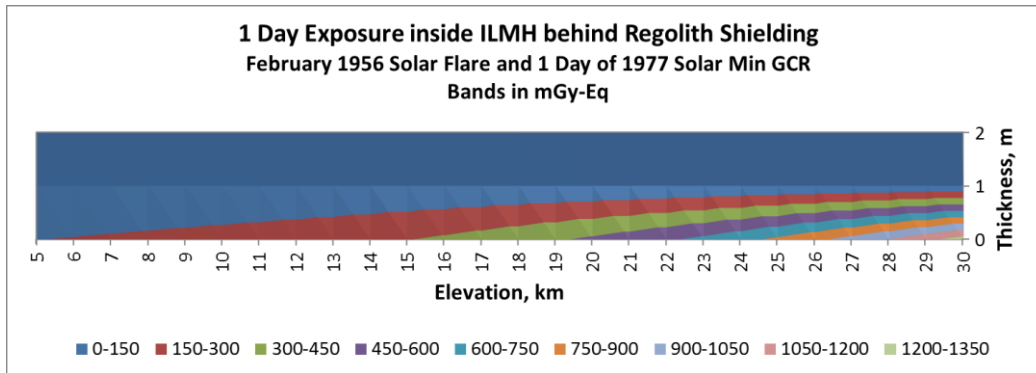International Conference on Environmental Systems

Figure 15. Contour plot of 1 day exposure inside ILMH – regolith shielding
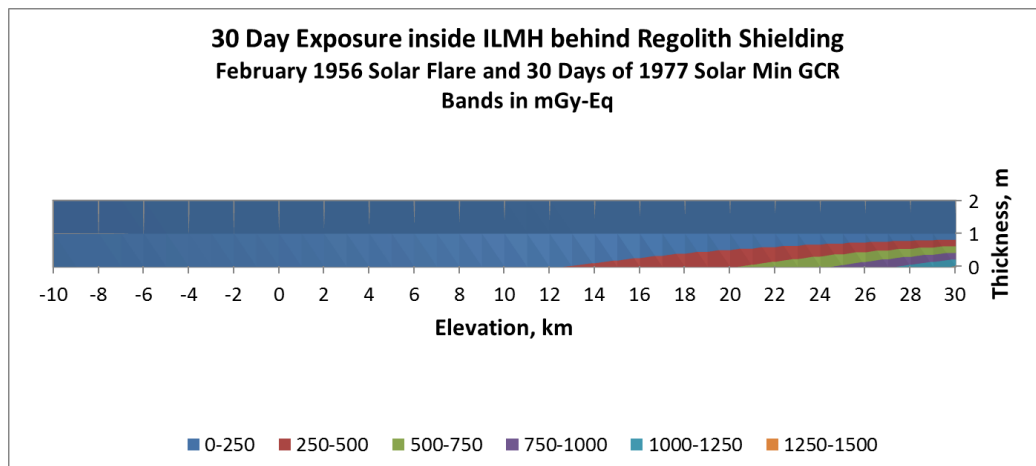

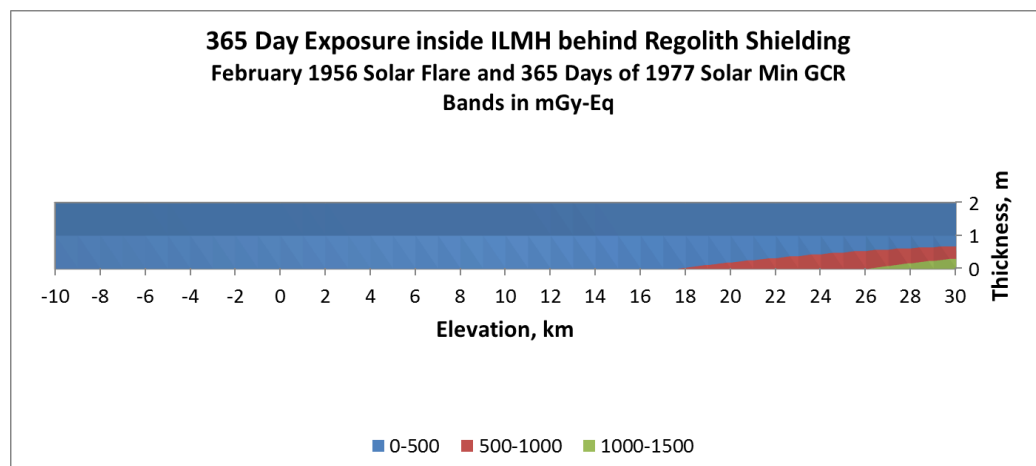**Figure 16. Contour plot of 30 day exposure inside ILMH – regolith shielding**

Figure 17. Contour plot of 365 day exposure inside ILMH – regolith shielding

B. PER

We calculated doses at the cockpit and sleep area (hammock) target points inside the PER at surface elevations from -10 to 30 km. Figures 18 and 19 are plots of acute exposure on the port and starboard sides, respectively. The doses are due almost entirely to the solar flare, with minimal contribution from GCR. Hence, the solar flare strongly

dominates the internal radiation environment. At 30 km, the dose at the port cockpit point in the external environment is 1269 mGy-Eq, which exceeds the 700 mGy threshold for acute radiation syndrome. Figure 18 indicates that the very light shielding of the thin PER shell reduces it to 665 mGy-Eq, which is about half of the external environment level. Figures 18 and 19 indicate dose is highest at the target points behind the cockpit windows, with a general, though small downward trend in dose at hammock target points in the bow-to-stern direction. This is not surprising, as the cockpit target points have minimal shielding behind large windows, while the hammock target points are behind the very light shielding of the PER shell, and at lower height than the cockpit windows. However, the downward trend in dose in the bow-to-stern direction is small, and it does not indicate existence of cold areas in the internal radiation field. Results do not support optimum repositioning of crew sleep areas. Interpolation of port cockpit doses indicates exposure exceeds 150 mGy-Eq above 5.5 km.

A cursory examination of Figures 18 and 19 indicates similar trends in dose on the port and starboard sides. However, there are slightly different trends on the port and starboard sides, due to the shielding asymmetry caused by the graphite epoxy hatch on the port side. Figure 20 shows HZETRN results for attenuation of SPE by hemispheres of fiberglass epoxy and graphite epoxy of 0.7 cm thickness, in the Mars surface environment. The plots indicate that fiberglass epoxy is a slightly better attenuator of SPE than graphite epoxy over the entire surface elevation range. Port target points have diminishing shielding behind graphite epoxy and increasing shielding behind fiberglass epoxy in the bow-to-stern direction, which impacts slightly the dose trend from SPE in the bow-to-stern direction. Since the starboard side is all fiberglass epoxy, there is a slight asymmetry in SPE dose trends between the port and starboard sides. Figure 21 shows HZETRN results for attenuation of GCR by hemispheres of fiberglass epoxy and graphite epoxy of 0.7 cm thickness, in the Mars surface environment. The plots indicate that graphite epoxy is a slightly better attenuator of GCR than fiberglass epoxy over the entire surface elevation range. Again, the asymmetry caused by the graphite epoxy hatch on the port side causes a small difference in trends of GCR dose between the port and starboard sides. Since the SPE environment is very dominant in acute exposure, trending for the total dose from SPE and GCR environments essentially follows the SPE trend.
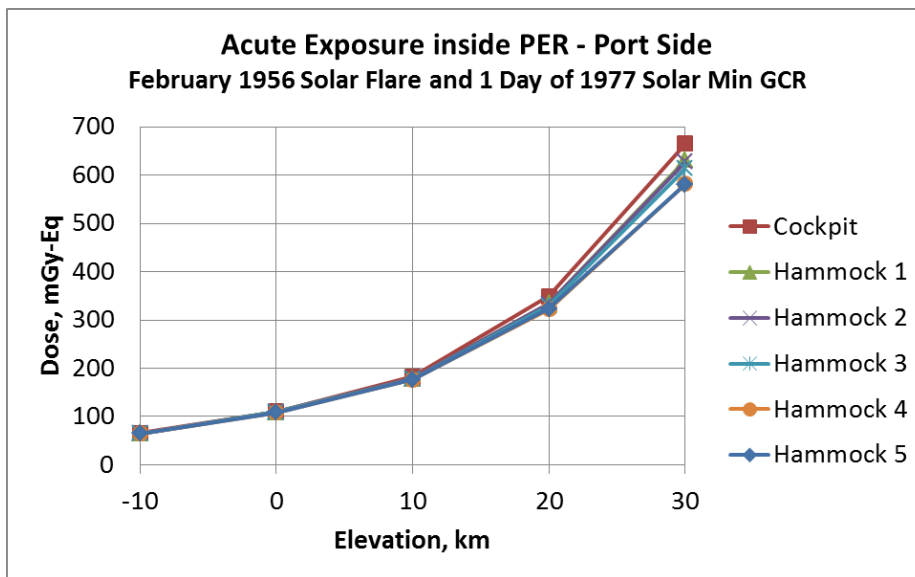

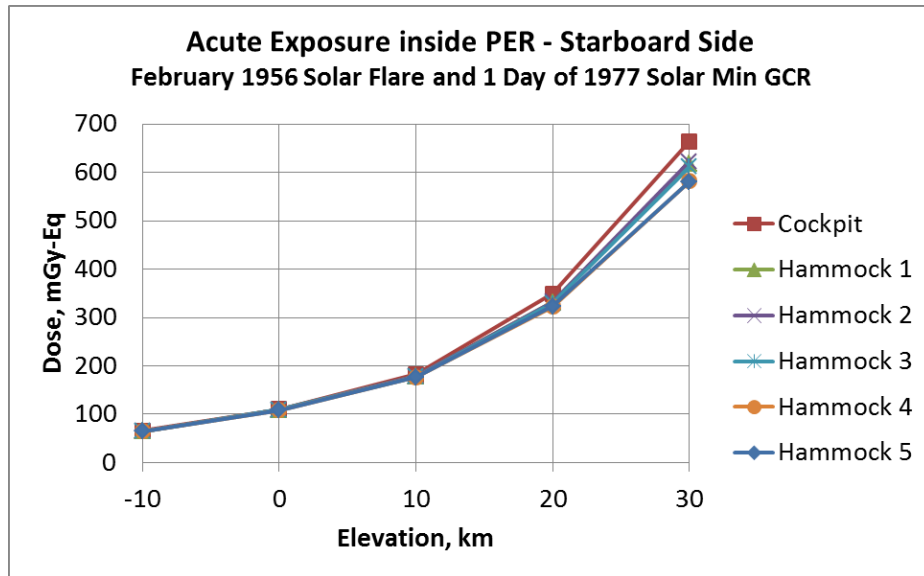**Figure 18. Acute exposure inside PER – port side**
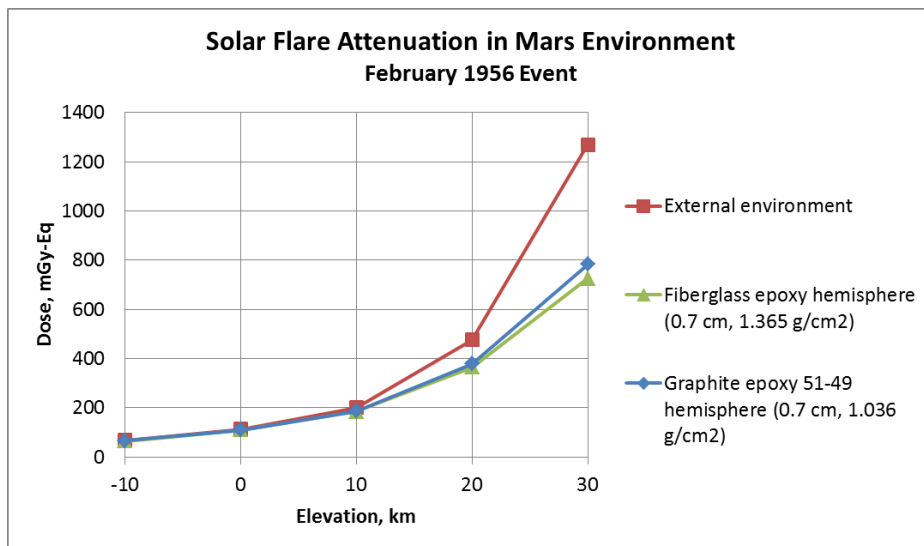
Figure 19. Acute exposure inside PER – starboard side

Figure 20. Solar flare attenuation by hemispheres in Mars environment

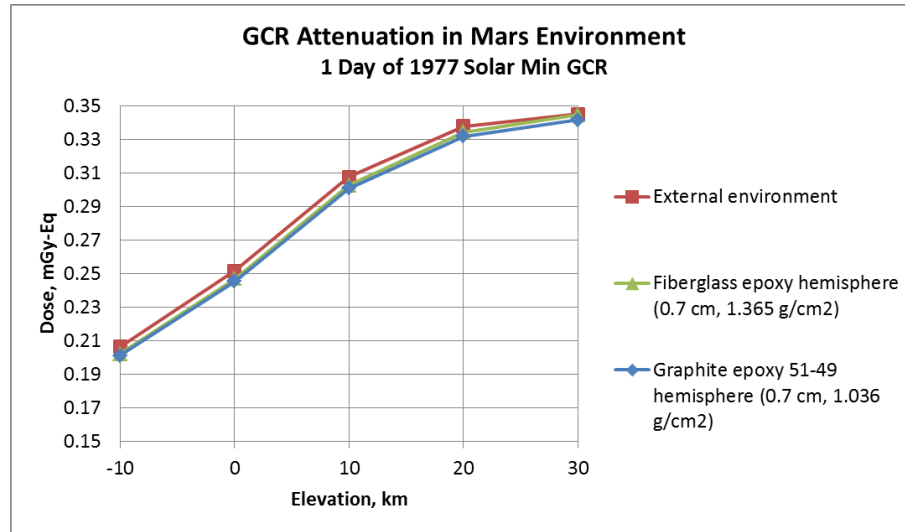International Conference on Environmental Systems

Figure 21. GCR attenuation by hemispheres in Mars environment

Figure 22 is a plot comparing acute exposure inside the baseline and heavy PERs on the port side over a surface elevation range of -10 to 30 km. It indicates higher attenuation inside the heavy PER, as expected, with similar trends in the bow-to-stern direction. For both the baseline and heavy PERs, the highest dose occurs at the cockpit target point. In the baseline PER, the port cockpit dose at 30 km is 665 mGy-Eq, while in the heavy PER it is 327 mGy-Eq, about half the level of the baseline PER. Hence, an almost fourfold increase in shielding reduced the dose only by about one half, indicating the diminishing effectiveness of increased shielding thickness.
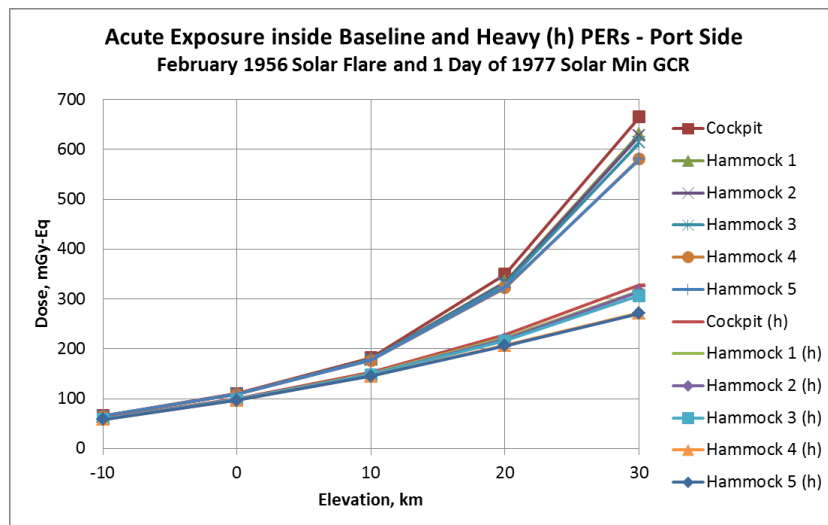

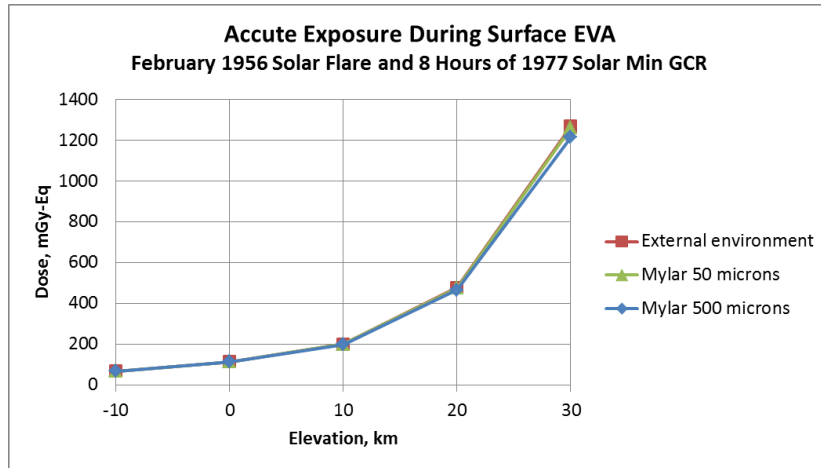**Figure 22. Acute exposure inside baseline and heavy PERs – port side**

International Conference on Environmental Systems

Figure 23. Acute exposure during surface EVA

C. Space Suit

We computed dose at the center of the Mylar hemisphere for acute exposure over a surface elevation range of -10 to 30 km. Figure 23 shows acute exposure during surface EVA, where the astronaut is protected only by the space suit fabric. The plots show doses in the external environment and under the protection of 50 and 500 micrometers of Mylar fabric. At only 8 hours of background GCR, the dose due to solar flare is strongly dominant, while the contribution from GCR is minimal. Results indicate there is minimal attenuation of radiation from the external environment level, even inside 500 micrometers of Mylar. Under 500 micrometers of Mylar, exposure exceeds 150 mGy-Eq at elevation above 4.3 km. The 700 mGy threshold for acute radiation syndrome is exceeded at elevation above 23.1 km.

D. Surface Scenarios

Total radiation exposure varied considerably over the three surface scenarios. Total exposures and acute exposures from the solar flare and background GCR during EVA are summarized in Table 5. Limits for 1 year exposure are met under the minimal and intermediate scenarios. Under the intermediate scenario, most of the 221 mGy-Eq total exposure is due to the solar flare that occurs at 4 km elevation while the astronaut is performing EVA under the protection of 500 micrometers of Mylar fabric. The total exposure to solar flare and GCR during this EVA is 139 mGy-Eq, which is below the 150 mGy-Eq limit. Under the extreme scenario, the 500 mGy-Eq limit for BFO and heart is exceeded. Most of the 1025 mGy-Eq total exposure is due to the 1 day mountain climb from 24 to 30 km elevation, where the solar flare occurs while the astronaut is performing EVA under the protection of 500 micrometers of Mylar fabric. Exposure during this EVA is 628 mGy-Eq, which is close to the threshold of 700 mGy for acute radiation syndrome. (Under all three scenarios, the 100 mGy limit for CNS at $Z \geq 10$ is met, since 1 year GCR exposure is below 100 mGy even at 30 km elevation.)

Table 5. Exposure for 365 day surface stay

Surface Scenario	Acute Exposure from Solar Flare and Background GCR during EVA (mGy-Eq)	Total Exposure (mGy-Eq)
Minimal	-	176
Intermediate	139	221
Extreme	628	1025

IV. Conclusions and Future Research Directions

A. ILMH

Selection of ILMH shielding material and thickness depends on the range of Mars surface elevation of interest for exploration. The severity of the radiation environment increases as surface elevation increases, due to decreasing protection provided by the atmosphere. In order to serve as the primary radiation storm shelter, the ILMH must meet the acute exposure limit, in addition to 30 and 365 day limits. In the external environment, these conditions are met at elevation below 5 km. At 5 g/cm^2 of polyethylene shielding, the conditions are met below 11 km. At 10 g/cm^2, the conditions are met below 18 km. Finally, at 15 g/cm^2, the conditions are met below 25 km. The maximum suggested surface elevations for deployment of the ILMH under unshielded conditions and under polyethylene shielding are summarized in Table 6.

There are no elevation restrictions behind 1m of regolith shielding. A 1m layer of Mars regolith provides adequate protection to remain below 150 mGy-Eq for acute exposure, and to meet all PELs for 30 day and 365 day exposure. A 2m layer of regolith reduces exposure to almost negligible levels. Use of Mars regolith offers the additional advantages of being available in situ, with associated payload mass and volume savings, and of being nonparasitic, as it can also provide thermal insulation and micrometeoroid protection.

Table 6.   Maximum surface elevation (km) for deployment of ILMH

Unshielded	Polyethylene Shielding		
	5 g/cm^2	10 g/cm^2	15 g/cm^2
5	11	18	25

Figure 24 is a diagram showing the ILMH under a layer of regolith. The figure shows the concept developed by the UND Department of Space Studies and colleagues specifically for lunar exploration, but seated on the Mars surface. The shield consists of a layer of sacks filled with regolith and stacked on top of each other. The weight will be supported by the fabric structure and transferred to the rigid frame through conjugation joints.[11] The ILMH has sufficient structural margin to support 1m of Mars regolith in the Mars gravitational environment of 0.376 g. In addition, the interior panels of the ILMH could be manufactured of polyethylene or another hydrogen-rich material, to provide additional shielding.

Further development of the ILMH is required to make it suitable as a long-term habitat on Mars. The next evolution of the ILMH could be an underground structure for a long term Mars base.
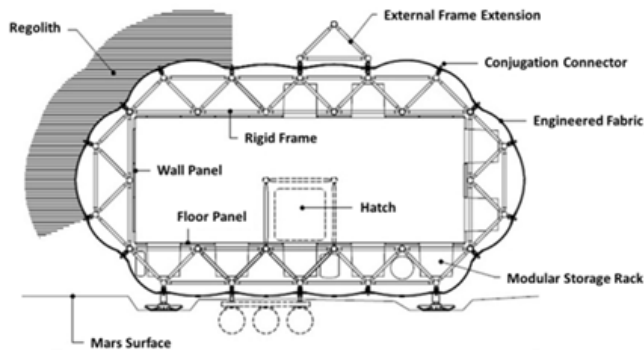

Figure 24. ILMH under a layer of regolith[11]

B. PER

The thin PER shell provides very limited protection from the external radiation environment. Without additional shielding, the PER cannot protect the crew from a February 1956 solar flare at elevation above 5.5 km, where exposure exceeds 150 mGy-Eq. At 30 km elevation, exposure is close to the threshold for acute radiation syndrome. In its current configuration, the PER will not serve as an adequate secondary storm shelter over most of the surface

elevation range. The dose trends noted in the bow-to-stern direction are small, and do not result in large variations in dose at any surface elevation. Therefore, they do not support development of an optimum configuration of sleep areas. Figures 20 and 21 show that fiberglass epoxy and graphite epoxy have similar attenuation effectiveness at the same thickness. Graphite epoxy 51-49 was already shown to be a good attenuator. Hence, the poor radiation protection provided by the PER is not due to its materials. It is due to the very thin shell. The baseline areal densities of fiberglass epoxy and graphite epoxy (1.365 and 1.036 g/cm^2, respectively) will not even provide minimal shielding. At a thickness of about 0.7 cm, no "realistic" material is likely to provide adequate attenuation. Selection of alternative materials will have minimal impact at this thickness. However, if the thickness of the shell is increased to provide radiation protection comparable to an adequately shielded ILMH, the PER becomes quite massive, requiring much more power for surface roving, which limits its performance envelope.

Strategies for radiation protection inside the PER are limited. The very tight space inside the PER would make adequate internal shielding unfeasible. Both internal and external shielding would cause interface problems. We recommend a strategy of early warning of increased solar activity, to alert the crew to drive back to the ILMH in time to escape a severe solar storm, or else park under the protection of natural topography, if there happens to be suitable topography nearby. A radiation monitoring device, like the Radiation Assessment Detector (RAD) instrument on the Curiosity Mars rover, could be installed at the ILMH site, with at least one astronaut remaining in the ILMH while up to three astronauts perform surface roving and EVA. The astronaut(s) inside the ILMH could monitor external charged particle activity and alert the others to return to the ILMH upon detection of increased charged particle counts. Since solar flares often have rise times of hours, this may give the astronauts time to return to the protection of the ILMH and escape the worst of the solar storm. However, after several hours of roving, the PER may be too far from the ILMH to return in time to escape a major solar flare, keeping in mind its top speed of 25 mph (along with possibly rough terrain) even with real-time warning of the flare. Since the crew may have to rely on local geological features for protection, initial surface exploration may be required just to perform surveys of local geological and survival resources. Radiation protection strategies for a future PER (or analogs) need to be redirected toward surface mission planning, utilization of surface features as protective shields, monitoring of space radiation environments, communication with an adequately shielded ILMH, and communication with mission control on Earth.

Another possibility is to redesign the PER and its power source to accommodate a heavier shell capable of providing adequate shielding for acute exposure, up to the maximum surface elevation of interest for exploration. Mass requirements were not included in the original PER design and construction, since radiation protection was not a primary goal at the time of rover design and construction. The initial goal was to develop a minimal planetary life support structure, to be followed eventually by further development of the concept to include radiation protection on the planetary surface, through proper mission design and deployment scenarios. It will be necessary to install a larger, more powerful battery to support mobility under the higher mass while also providing capacity for the planned scope of surface operations.

C. Space Suit

During a major solar storm, space suits provide negligible protection from radiation. Even under protection of 500 micrometers of Mylar fabric, there is minimal attenuation from the external environment level. At elevation above 4.3 km, exposure exceeds 150 mGy-Eq; at elevation above 23.1 km, exposure exceeds the threshold for acute radiation syndrome. We concluded that space suits will not provide protection from an event such as the February 1956 solar flare at any operationally realistic thickness or choice of space suit material. If there is no natural topography that may serve as a storm shelter, then surface EVA may have to be restricted to a very short distance from a shielded habitat, or to surface elevation below 4 km. This also drives the need to implement an early warning system for solar storms, to alert astronauts to return immediately to the protection of the habitat.

The radiation protection deficiency of space suits is due to their being very thin. Even at 500 micrometers, the shielding areal density of Mylar is only 0.0665 g/cm^2, which is two orders of magnitude below even minimal shielding of 5 g/cm^2. Hence, a spacesuit would have to be about 100 times as thick or as dense to provide even light shielding. Even so, light shielding is inadequate over a major portion of Mars surface elevation range, as we saw with the ILMH. In addition, issues related to the physiological part of human factors will make very heavy space suits impractical.

There is interest in use of metallized materials as space suit fabric. However, Townsend and colleagues already demonstrated the shielding inadequacy of a space suit modeled as an aluminum hemisphere at an areal density of 0.3 g/cm^2, during a worst case SPE on Mars.[10] A space suit made of aluminum of sufficient thickness ($\gg 5$ g/cm^2) would be massive. When the total weight of the suit is accounted for, it becomes impractical for an astronaut to

perform surface EVA regimens weighted by such a massive suit. Furthermore, at any operationally realistic weight, the degree of metallic content in suits will be far short of even minimal shielding.

D. Surface Scenarios

The surface scenarios indicate astronaut vulnerability to solar flare exposure during EVA, especially at high surface elevation, where the limited protection provided by the atmosphere is lowest. Outside the protection of a shielded habitat, exposure during a major solar flare above a few kilometers in elevation will likely be excessive. In the extreme scenario, where the flare occurs at the higher end of the elevation range, the acute exposure level approaches the threshold for acute radiation syndrome. Except for a restricted surface elevation range, there is no adequate protection from a major solar flare during EVA. Medical procedures for recovery from excessive radiation exposure need to be developed for implementation on the surface, and need to be integrated with mission deployment scenarios and performance of surface excursions. It is advisable to include a medical expert in the surface crew.

E. Future Research Directions

Radiation shielding analysis of UND planetary surface exploration concepts has progressed from analysis of planar incidence on flat shielding on the lunar surface, with no accounting for neutron backscatter[11], to multi-directional incidence on three-dimensional shielding on the Martian surface, with neutron backscatter, as performed in these investigations. So far, only very simple models of the habitat, rover, and space suit have been implemented for radiation analysis. The next logical progression should be in-depth analysis with vastly more detailed shielding thickness distributions, which will enable inclusion of internal structural members and hardware into the thickness distributions. This will generate more realistic modeling of habitat and rover shielding, with inclusion of internal shielding provided by walls, hardware, equipment, and fluid tanks.

In-depth analysis of human biological responses to space radiation requires use of the whole body equivalent dose method, with Computerized Anatomical Male (CAM) and Computerized Anatomical Female (CAF) phantom proxies integrated into the shielding thickness distributions.[12] This will enable five-zone (head, chest, pelvis, thighs, and calves) full body effective dose calculations, and can yield doses for individual organs. Researchers in stochastic radiation effects may prefer results for individual organs, as inputs to models for prediction of delayed responses to radiation exposure.

Acknowledgments

References

[1]NASA, "Space Flight Human System Standard, Volume 1: Crew Health," NASA-STD-3001, 2009, p. 67

[2]THREE, http://three.usra.edu/articles/AstronautRadLimitsFC.pdf, accessed 1 October 2014

[3]Singleterry, R. C., Blattnig, S. R., Clowdsley, M. S., Qualls, G. D., Sandridge, C. A., Simonsen, L. C., Norbury, J. W., Slaba, T. C., Walker, S. A., Badavi, F. F., Spangler, J. L., Aumann, A. R., Zapp, E. N., Rutledge, R. D., Lee, K. T., and Norman, R. B., "OLTARIS: On-Line Tool for the Assessment of Radiation in Space," NASA/TP-2010-216722, 2010

[4]Borggräfe, A., Quatmann, M., and Nölke, D., "Radiation protective structures on the base of a case study for a manned Mars mission," *Acta Astronautica*, 65, 2009, pp. 1292-1305

[5]Wilson, J. W., Townsend, L. W., Schimmerling, W., Khandelwal, G. S., Khan, F., Nealy, J. E., Cucinotta, F. A., Simonsen, L. C., Shinn, J. L., and Norbury, J. W., "Transport Methods and Interactions for Space Radiations," NASA Reference Publication 1257, 1991, p. 103

[6]Shinn, J. L. and Wilson, J. W., "An Efficient HZETRN (A Galactic Cosmic Ray Transport Code)," NASA Technical Paper 3147, 1992, pp. 1-2

[7]Townsend, L. W, Cucinotta, F. A., and Heilbronn, L. H., "Nuclear model calculations and their role in space radiation research," *Advances in Space Research*, Volume 30, Number 4, 2002, pp. 907-916

[8]Vashenyuk, E. V., Balabin, Y. V., and Miroshnichenko, L. I., "Relativistic solar protons in the ground level event of 23 February 1956: New study," *Advances in Space Research*, 41, 2008, pp. 926–935

[9]Badavi, F. F., Wilson, J. W, and Hunter, A., "Numerical study of the generation of linear energy transfer spectra for space radiation applications," *Advances in Space Research*, 47, 2011, pp. 1608-1615

[10]Townsend, L. W., Anderson, J. A., Adamczyk, A. M., and Werneth, C. M., "Estimates of Carrington-class solar particle event radiation exposures as a function of altitude in the atmosphere of Mars," *Acta Astronautica*, 89, 2013, pp. 189-194

[11]Schneider, I., Daga, A., de León, P., and Harris, G. (2010), "Interim Report for the Human Exploration of the Moon and Mars: Space radiation protection and mitigation strategies for a long term duration lunar base (a NASA funded study)," *40th International Conference on Environmental Systems*, CP6220, AIAA, Washington, DC, 2010, DOI/ISBN 10.2514/6.2010-6220

[12]Singleterry, R. C., Blattnig, S. R., Clowdsley, M. S., Qualls, G. D., Sandridge, C. A., Simonsen, L. C., Slaba, T. C., Walker, S. A., Badavi, F. F., Spangler, J. L., Aumann, A. R., Zapp, E. N., Rutledge, R. D., Lee, K. T., Norman, R. B., and Norbury, J. W., "OLTARIS: On-line tool for the assessment of radiation in space," *Acta Astronautica*, 68, 2011, pp. 1086-1097